Frontiers of Information Technology & Electronic Engineering
www.jzus.zju.edu.cn; engineering.cae.cn; www.springerlink.com
ISSN 2095-9184 (print); ISSN 2095-9230 (online)
E-mail: jzus@zju.edu.cn

1.3-μm 4×25-Gb/s hybrid integrated TOSA and ROSA*

Yu LIU[†1,2], Hao-tian BAO[†1,2], Yi-ming ZHANG[1,2], Zhi-ke ZHANG[3],
Yun-shan ZHANG[4], Xiang-fei CHEN[4], Jun LU[4], Yue-chun SHI[4],
Jia-shun ZHANG[1,2], Liang-liang WANG[1,2], Jun-ming AN[1,2], Ning-hua ZHU[1,2]

[1]*State Key Laboratory on Integrated Optoelectronics, Institute of Semiconductors, Chinese Academy of Sciences, Beijing 100083, China*
[2]*School of Electronic, Electrical and Communication Engineering, University of Chinese Academy of Sciences, Beijing 100049, China*
[3]*State Key Laboratory of Advanced Optical Communications System and Networks,*
School of Electronics Engineering and Computer Science, Peking University, Beijing 100871, China
[4]*Microwave-Photonics Technology Laboratory, College of Engineering and Applied Sciences, Nanjing University, Nanjing 210093, China*
[†]E-mail: yliu@semi.ac.cn; bht@semi.ac.cn

Received July 4, 2018; Revision accepted Sept. 9, 2018; Crosschecked Apr. 11, 2019

Abstract: The design and fabrication of a compact and low-cost 4×25-Gb/s transmitter optical sub-assembly (TOSA) and receiver optical sub-assembly (ROSA) using a hybrid integrated technique are reported. TOSA and ROSA are developed without thermoelectric cooler for coarse wavelength division multiplexing applications. Physical dimension of the packaged optical sub-assembly is limited to 11.5 mm×5.4 mm×5.4 mm. The design of TOSA and ROSA is employed using a silica-based arrayed waveguide grating chip to select the specific channel wavelength at O-band. In TOSA, the wavelength of four 1.3-μm discrete directly modulated laser chips is well controlled based on the reconstruction equivalent chirp technique. In the back-to-back transmission test, bit error rates for all lanes of cascade of the TOSA and ROSA are small. A clear opening eye diagram is obtained.

Key words: Reconstruction equivalent chirp; Arrayed waveguide grating; Transmitter optical subassembly; Hybrid integrated
https://doi.org/10.1631/FITEE.1800371 **CLC number:** TN24

1 Introduction

Optical metro and core network play a significant role in supporting Internet data transmission. The emergence of new bandwidth-hungry services and new broadband access technologies is promoting dynamic growth in Internet traffic (Baek et al., 2012). To accommodate ultra-high bandwidth traffic, several 100-Gb/s Ethernet standards were formulated in 2010. Since then, there has been a lot of research in achieving 100-Gb/s transmission (Dong et al., 2014; Machado et al., 2014). Wavelength division multiplexing (WDM) and improving the single-channel data rates are two main methods. Considering the feasibility of the technique and economic benefits, multi-lane approaches were the good way to realize large transmission (Kanazawa et al., 2016; Zhao et al., 2016; Zhong et al., 2017).

Distributed feedback (DFB) multi-wavelength semiconductor laser arrays (MWLAs) integrating several lasers with different wavelengths on one carrier have played a significant role in optical communication. Electron beam lithography (EBL) has been the most commonly used method to fabricate MWLAs over the last 20 years. However, the wavelength accuracy of laser chips cannot be guaranteed. The reconstruction equivalent chirp (REC) technique is a promising way to fabricate MWLAs (Zhang et al.,

* Project supported by the National Natural Science Foundation of China (Nos. 61635001 and 61575186) and the National High-Tech R&D Program of China (863 Program) (No. 2013AA014201)
ORCID: Hao-tian BAO, http://orcid.org/0000-0003-0831-8841

2017). Compared with other methods, it can simplify the fabrication steps, and the wavelength accuracy can be precisely increased by 100 times. Dai and Chen (2007) used the REC technique to fabricate a single DFB laser chip. Then it was quickly used to fabricate MWLAs.

Because of the wide and flat spectral response and low transmission loss, thin-film filters (TFFs) with a free-space structure were used as the demultiplexer (DEMUX) in multi-wavelength systems (Kang et al., 2010). InP-based or silicon-on-insulator photonic integrated circuit and planar light-wave circuit (PLC) hybrid integration were extensively studied. The silica-on-silicon-based arrayed waveguide grating (AWG) PLC hybrid integrated technology found its commercial applications, because of its advantages of low-loss multiplexing, low-cost assembly, and compact size. It has become a practical solution competitive with other integration technologies (Dai et al., 2014).

The hybrid integrated technique, in which many discrete chips are mounted on one common subcarrier, offers many advantages, such as low cost and being optional and simple. The Nippon Telegraph and Telephone (NTT) developed compact hybrid integrated transmitter optical sub-assembly (TOSA) and receiver optical sub-assembly (ROSA) with AWG for 100-Gb/s communication (Doi et al., 2015). However, there are some differences. Electro absorption modulator integrated distributed feedback (EADFB) and thermoelectric cooler (TEC) were used in TOSA, increasing energy cost and complexity (Ohyama et al., 2016). In ROSA, the back-side-illumined photodetector (PD) arrays were flip-chip mounted on the ceramic carrier to guarantee that light transmission from the AWG to PD would not change (Doi et al., 2015). Although the AWG chip was used as the multiplexing/demultiplexing, compared with TOSA/ROSA we have developed, there are many differences.

The design and fabrication of DFB laser array chips based on the REC technique and multi-mode AWG chip were discussed. Then we detailed the fabrication of TOSA and ROSA modules using the hybrid integrated technology, including the design of optical coupling and radio frequency (RF) circuit. Moreover, the measured 3-dB bandwidth of TOSA was 3 GHz, and 10-dB bandwidths of all lanes exceeded 15 GHz.

2 Design and fabrication of the distributed feedback (DFB) laser array chip

DFB laser array is one of the most important components in the hybrid integrated 100-Gb/s TOSA. It is a difficult task to fabricate a DFB laser array with all wavelengths meeting the requirement of the WDM. Using the REC technique, we developed a four-channel DFB laser array with high wavelength accuracy for coarse wavelength division multiplexing (CWDM) systems.

The four-channel DFB laser array is shown in Fig. 1. The cavity length of the DFB laser array was 250 μm with a common ridge waveguide structure. Gratings in the four-channel DFB laser array had a $\lambda/4$ phase shift (EPS) at the center. Seed grating period Λ_0 was set to 214.83 nm, while the sampling periods P_n (n=1, 2, 3, 4) of the four lasers were 2.31, 2.87, 3.75, and 5.36 μm, respectively. Designed wavelength spacing of the four-channel DFB laser array was 20 nm.

Fig. 2a shows the spectra of the four lasers. All lasers operated in a good single-longitudinal mode (SLM) state. Wavelengths and linear fitting curve of the DFB laser array are shown in Fig. 2b. Wavelengths of the four channels were 1268.8, 1288.9, 1308.7, and 1328.6 nm, respectively. Measured average wavelength spacing obtained from the linear fitting curve was 19.92 nm, which was only 0.08 nm smaller than the designed value. Temperature drift coefficients of the laser wavelengths in all channels were basically the same, all near 0.1 nm/°C. As shown in Fig. 3, the wavelength shift ratio of lane 3 was 0.092 nm/°C.

Power-current (*P*-*I*) curves of different lasers in the laser array at room temperature are shown in Fig. 4. All the threshold currents were nearly 5 mA.

3 Design and fabrication of arrayed waveguide grating (AWG) chip

3.1 4×25-Gb/s AWG MUX chip with 1.3-μm CWDM

Fig. 5 shows the diagram of the four-channel AWG CWDM chip, which had four input ports and one output port, and each input channel was on the CWDM grid with 20-nm wavelength spacing from 1271 to 1331 nm. In addition, the wavelength of the

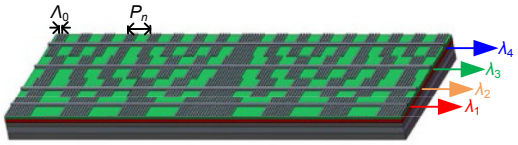

Fig. 1 Four-channel distributed feedback (DFB) laser array for coarse wavelength division multiplexing (CWDM) systems

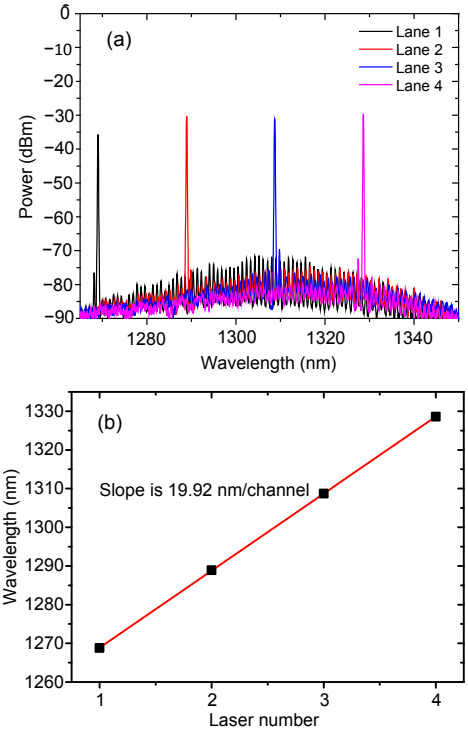

Fig. 2 Spectra (a) and wavelengths and linear fitting curve (b) of the four-channel DFB laser array
References to color refer to the online version of this figure

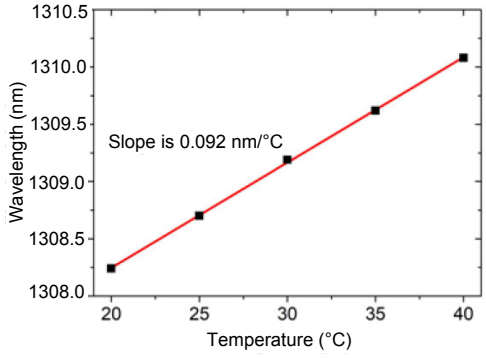

Fig. 3 Wavelength shift ratio of lane 3

AWG would have been red-shifted if the temperature rose. The red-shift coefficient was 0.011 nm/°C. To decrease the CWDM chip size, the refractive index difference between the core and cladding was processed as 2.0%, which would decrease the waveguide

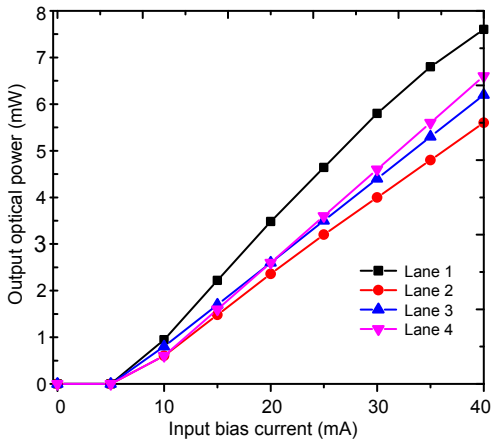

Fig. 4 Measured power-current (*P-I*) curves of the laser

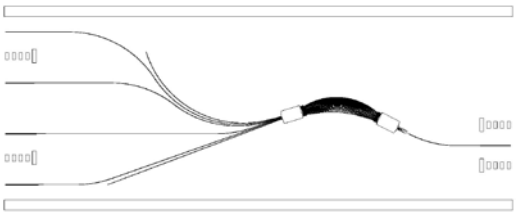

Fig. 5 Diagram of the four-channel AWG CWDM chip

bend radius to 1.5 mm without increasing insertion loss. The core size of the input and output waveguides was 4.5 μm×4.5 μm for the single-mode condition. According to the AWG diffraction equation, key parameters were obtained (Table 1). The 0.75-mm pitch of input waveguides was designed for convenient coupling between directly modulated lasers (DMLs) and microlenses. The AWG CWDM chip size was 8.3 mm×3.7 mm. A pigtail fiber was butt-coupled to the output waveguide of the AWG.

Table 1 Key parameters of the four-channel AWG CWDM

Parameter	Symbol	Value (μm)
Center wavelength	λ_0	1.3
Wavelength spacing	$\Delta\lambda$	0.02
Array waveguide spacing	d	6
Output waveguide spacing	Δx_0	7
Adjacent array waveguide length difference	ΔL	7.09
Roland circle diameter	R	630

The designed four-channel CWDM AWG was fabricated using a standard semiconductor process. The SiO_2-GeO_2 core with a thickness of 4.5 μm was

deposited on a silicon substrate with a thickness of 15 μm silicon dioxide undercladding by plasma enhanced chemical vapor deposition (PECVD). Contacting photolithography was used for pattern transfer. The core with a width of 4.5 μm was etched using the inductively coupled plasma (ICP) etching method. Upper cladding silica with boron (B) and phosphorus (P) doping was deposited by PECVD. The fabricated AWG chip was diced from wafer, and the end faces of the input and output waveguides were polished to 8° to reduce the optical return loss. Optical performance of the AWG CWDM was measured with an O-band tunable light source, a polarization controller, and optical detectors. As shown in Fig. 6, the central wavelengths of Ch1, Ch2, Ch3, and Ch4 were 1270, 1290, 1310, and 1330 nm, respectively, agreeing well with the theoretical design. The peak insertion loss was less than 2.5 dB, and the 1-dB bandwidth was larger than 10 nm, satisfying assembly requirements. The output waveguide of an AWG CWDM was coupled with a pigtail fiber which introduced a 0.5-dB coupling loss.

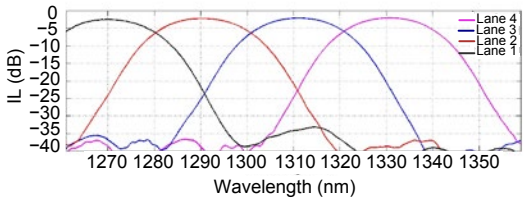

Fig. 6 Measured output spectra of the AWG CWDM
Black, red, blue, and purple lines represent Ch1, Ch2, Ch3, and Ch4, respectively. References to color refer to the online version of this figure

3.2 4×25-Gb/s AWG DEMUX chip with 1.3-μm CWDM

Usually, the input and output waveguides of an AWG are single-mode structures. However, AWG chips in ROSA packages have multi-mode output waveguides, which can provide a broad flat-top spectral profile. The wavelength of a laser will drift because of direct modulation (frequency chirp) and active layer temperature changing; therefore, the box-like spectra can provide a much larger receiving tolerance. To obtain a more compact device rather than the waveguides with 0.75% and 1.5% index contrast, the rectangle doped-silica waveguides with 2% refractive index contrast were adopted. We first chose the height of the core waveguides to be 4 μm, considering the optical confinement factor and ability to manufacture. The relationship between the waveguide width and effective refractive index is shown in Fig. 7. To confirm the mode condition of all wavelengths, we chose 1271 and 1331 nm for simulation, which were the smallest and largest wavelengths specified in IEEE 802.3 ba.

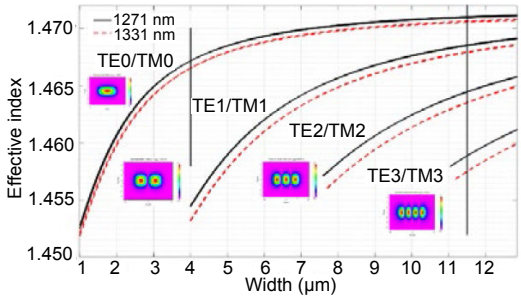

Fig. 7 Relationship between the waveguide width and effective refractive index (n_{eff})

We can see that all wavelengths had the same mode quantity, and we set the single- and multi-mode waveguide widths as 4 and 11.5 μm, respectively. Four modes existed in such multi-mode waveguides.

Light transmission direction in the AWG waveguides was horizontal, but the PD's absorption area was on the top, which means that a light turning component was needed to change the direction from horizontal to vertical. To simplify the coupling process, the end facet of output waveguides was directly ground at a certain angle (i.e., 40°) as a total internal-reflection mirror to change the direction. Three-dimensional (3D) finite-difference time-domain (FDTD) method was adopted to simulate the total reflection mirror (Fig. 8).

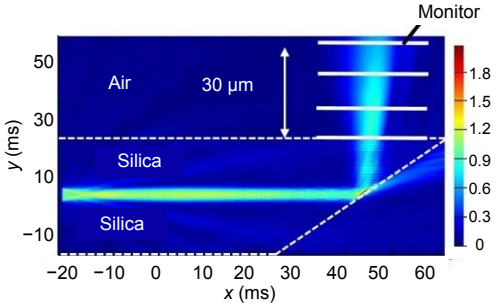

Fig. 8 Longitudinal section of the propagation simulation with an angle of 40°

The AWG chip was fabricated by silica. First, the lower silica cladding was grown on the silicon

substrate. Then PECVD was used to deposit the germanium-doped layer. Next, the waveguide structure was formed by the ICP etching method, making edges smooth and sharp. Finally, the silica upper cladding was grown again by PECVD.

To reduce the reflection loss, the AWG chip will be flipped over when coupling with the PD array; therefore, light needs to pass through only the thin upper cladding of the AWG. Turning mirror was made in several steps: First, the end facet of waveguides was roughly ground by grinder; Then we used SiC particles with 1-μm diameter to polish 30 min; Last, CeO_2 particles with 0.5-μm diameter were used to further polish another 30 min, which makes the mirror extremely smooth and minimizes the reflection loss (Li et al., 2018).

4 Hybrid integrated TOSA and ROSA

Based on the studies of directly modulated DFB lasers with multi-wavelength and AWG chips, mentioned in Sections 2 and 3, we fabricated the 4×25-Gb/s TOSA/ROSA using a hybrid integrated technique. Back-to-back (BTB) transmission performances were verified.

4.1 TOSA

As shown in Fig. 9, many active and passive photonic devices were packaged in a compact ceramic cuboid shell. The size of the package housing is 11.5 mm×5.4 mm×5.4 mm. Because the pitch of laser chips on the monolithic laser array is fixed, it is impossible to laterally adjust the optical path, leading to a decrease of coupling efficiency. The DFB laser array (MWLA) chip with different operational wavelengths of 1269.5, 1289.7, 1309.6, and 1329.7 nm was cleaved into four discrete lasers, which were installed on an RF circuit board. A four-channel silica-based AWG chip was mounted on the substrate to multiplex different optical signals into one fiber because of its low dimension and sufficient wavelength spacing. Four focusing lenses were placed between laser chips and AWG to improve the optical coupling efficiency.

The 3-dB bandwidth of the RF circuit board, which connects the DML chips and external circuitry, will influence the transmission performance. The matching impedance and suppression of crosstalk between different channels should be focused on. The impedance of the transmission line should meet the requirement of the 50-Ω measure system. Signal line width and gap distance between the center conductor and coplanar ground plane were set to 0.09 and 0.04 mm, respectively, while the isolation layer was made of 0.25-mm AlN. Four 40-Ω matching resistors were used to compensate for the 10-Ω laser load. An Au film was deposited on the back and top surfaces of the AlN ceramic by the electroplating method. Three sidewalls of the RF circuit were metalized to connect the ground of top and lower surfaces.

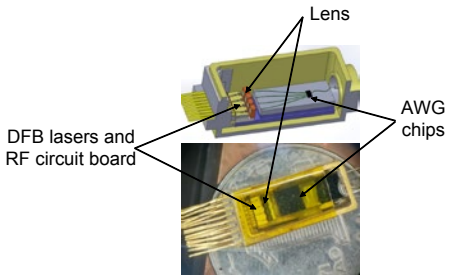

Fig. 9 Comparison of schematic and physical maps for the 4×25-Gb/s TOSA module

Fig. 10 shows the S21 curves of the microwave circuit, in which the insertion losses for four lanes from DC to 30 GHz were about 1.7, 1.3, 1.3, and 1.5 dB, respectively. The 2.5-dB decreasing value was caused by the matching resistor. In addition, the electrical crosstalk of adjacent channels was less than −20 dB.

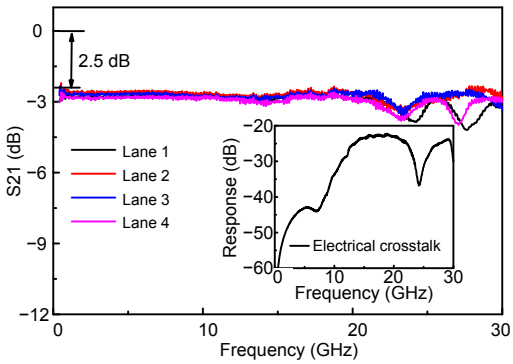

Fig. 10 S21 curves and electrical crosstalk for the microwave circuit board
References to color refer to the online version of this figure

Fig. 11 demonstrates how the laser ships and RF circuit fit together. The negative (N) electrode of the laser chip was directly set and soldered on the shared

ground line of the RF board, while the positive (P) electrode connected with the signal line through the golden bonding wire. Because lateral alignment was critical for reducing the mismatch, alignment marks were fabricated at the proper location on the RF circuit, guaranteeing that the transverse pitches of laser chips and lens were both 0.75 mm.

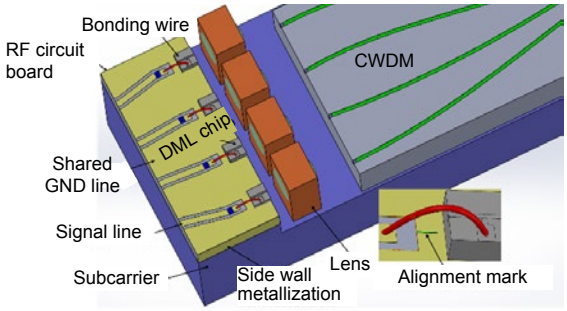

Fig. 11 Connection between laser chips and RF circuit

Stable and precise optical coupling is essential for low-loss and high-bit-rate communication systems. Nevertheless, with the mismatch between DFB laser and waveguide modal profiles (spot sizes), a simple butt-joint method will result in poor coupling efficiency, typically 10%. The employment of a lens to make the divergent light beam converge is completely necessary. The focus point was determined by a simulation of the sequential raytracing method. We could ultimately find that the distances from the laser chip and input waveguide to the facet of the lens were 0.21 mm and 0.518 mm, respectively. As Fig. 12 shows, the total gap between the DML chip and facet of the waveguide was 1.24 mm using a 0.5-mm lens. In addition, carefully adjusting the height of the subcarrier of individual optical devices to ensure their center in the same plane could increase the concentricity accuracy. The coupling efficiency could be increased to 80% after optimization.

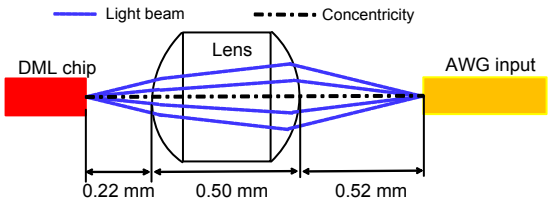

Fig. 12 Optical coupling diagram

Fig. 13 shows the *P-I* curves of the TOSA module. It indicates that when the injected current was 40 mA, the output optical power of all channels was larger than 2.5 mW. All wavelengths were within the range of the CWDM grid. Side-mode suppression ratios (SMSRs) in all lanes were larger than 40 dB (Zhang et al., 2018).

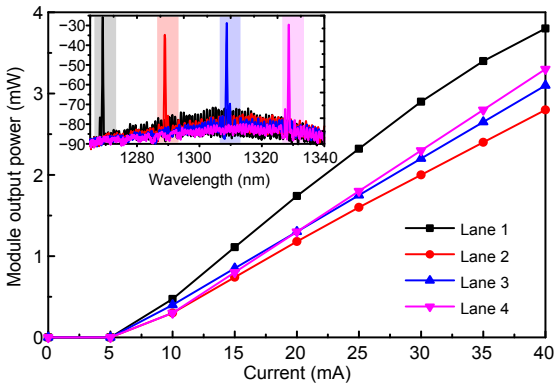

Fig. 13 *P-I* curves of TOSA and the spectrum of DML
Colored areas of the insert graph refer to the CWDM grid. References to color refer to the online version of this figure

4.2 ROSA

ROSA consists of three portions, including a silica-based PLC AWG chip, a four-channel mesa-type PIN PD array, and a microwave circuit board. The package of the receive module is similar to that of the transmitter module. Fig. 14 shows the 4×25-GHz ROSA. The AWG chip allocated the optical signals from fiber into four specific wavelengths, which were collected and transformed to electric signals by the four-channel PD array. High responsivity of a normal mesa-type Ge/Si PIN PD made it suitable for hybrid integration. The diameter of the absorption area was 20 μm. The responsivity could reach 0.9 A/W@−3 V, and normal dark current was 150 nA@−3 V. The PD array was mounted on the carrier according to the upward direction of the photosensitive face. The output side end facet of the AWG, which was located above the photosensitive face, was polished to form a 40° mirror. Thus, the direction of the laser light in AWG could be turned to illuminate the PD without using any light turning component. Tungsten copper alloy coated with Au was chosen as the chip sink, because of its outstanding thermal conductivity, dielectric constant, and the fact that its thermal expansion coefficient matches the Si-Ge material well. The AWG chip and PD array were actively aligned and coupled in the hybrid integrated process. The PD

array was stuck to a carrier by conductive epoxy. The AWG chip was held and moved by a fixture toward the PD array until the PD produced the maximum photocurrent. Then the AWG chip was adhibited with UV glue.

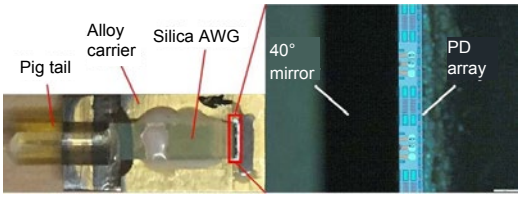

Fig. 14 Photograph of the 4×25-GHz ROSA

High-speed characteristic of transmission linking with TOSA and ROSA was measured. Fig. 15 shows the 28-Gb/s experimental setup. To achieve an identical optical power output, the bias current for lanes 2–4 was set to 35 mA, while the bias current of lane 1 was 30 mA. The output power was about 2.5 mW (Fig. 13). 28-Gb/s, non-return to zero (NRZ), and $2^{31}-1$ pseudo-random bit sequence (PRBS) signals were generated by a bit pattern generator (BPG). Before introducing the laser, the output signal from the BPG was amplified by the electric amplifier (EA), whose 3-dB bandwidth exceeded 38 GHz. ROSA was used to receive and convert the modulated optical signal to an RF signal, which was recorded by a real-time 100-GSa/s digital sampling oscilloscope (DSO) and processed off-line.

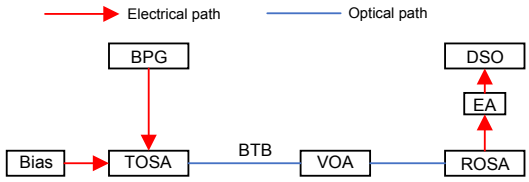

Fig. 15 28-Gb/s back-to-back (BTB) transmission of TOSA and ROSA

BPG: bit pattern generator; EA: electric amplifier; VOA: variable optical attenuator; DSO: digital sampling oscilloscope

Fig. 16 shows the bit error rates (BERs) between TOSA and ROSA. When performing the BTB transmission experiment, the sensitivities of the receiver for lanes 1–4 at the forward error correction (FEC) limited to 5×10^{-5} were about −7.1, −6.6, −6.2, and −5.1 dBm, respectively. Fig. 17 shows the obtained eye diagrams, which were very clear without overshoots or ripples.

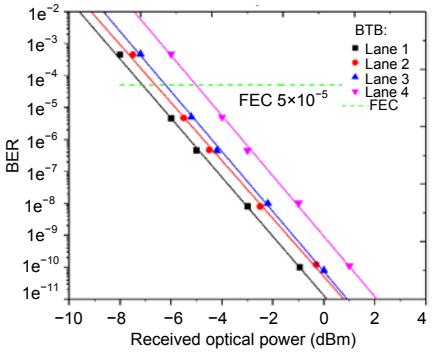

Fig. 16 Bit error rates (BERs) between TOSA and ROSA under 28-Gb/s operation

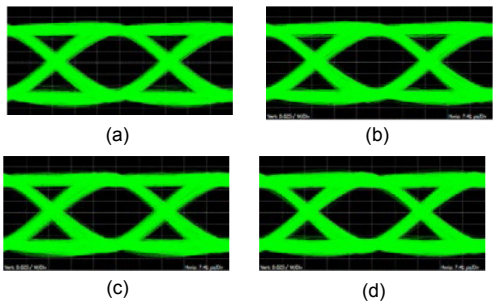

Fig. 17 Eye diagrams of four channels under 28-Gb/s operation for back-to-back (BTB) transmission: (a) lane 1; (b) lane 2; (c) lane 3; (d) lane 4

5 Conclusions

In this study, the 4×25-Gb/s TOSA and ROSA have been fabricated to realize 100-Gb/s transmission. Using the REC technique, an accurate wavelength DFB laser array has been fabricated. The developed AWG chip with multi-mode structure and broad flat-top spectral profile can provide sufficient wavelength spacing to enable the laser to operate without TEC. For packaging, to facilitate the adjustment of optical path and enhance the coupling efficiency, the monolithic DFB laser array has been cleaved into four discrete laser chips. Four chips have been packaged with four lenses and one AWG chip operating on the O-band in a compact ceramic packaging housing. RF board has been side-metalized to suppress crosstalk. The measured 3-dB bandwidth of TOSA was 3 GHz, and the 10-dB bandwidth exceeded 15 GHz. The performance of 100-Gb/s BTB transmission from TOSA to ROSA was good. The long-distance transmission performance of the proposed TOSA and ROSA will be discussed in the future.

References

Baek Y, Han YT, Lee CW, et al., 2012. Optical components for 100G ethernet transceivers. Proc 17th Opto-Electronics and Communications Conf, p.218-219. https://doi.org/10.1109/OECC.2012.6276449

Dai HQ, An JM, Wang Y, et al., 2014. Monolithic integration of a silica-based 16-channel VMUX/VDMUX on quartz substrate. *J Semicond*, 35(10):104010. https://doi.org/10.1088/1674-4926/35/10/104010

Dai YT, Chen XF, 2007. DFB semiconductor lasers based on reconstruction-equivalent-chirp technology. *Opt Expr*, 15(5):2348-2353. https://doi.org/10.1364/OE.15.002348

Doi Y, Oguma M, Yoshimatsu T, et al., 2015. Compact high-responsivity receiver optical subassembly with a multimode-output-arrayed waveguide grating for 100-Gb/s Ethernet. *J Lightw Technol*, 33(15):3286-3292. https://doi.org/10.1109/JLT.2015.2427367

Dong P, Liu X, Chandrasekhar S, et al., 2014. Monolithic silicon photonic integrated circuits for compact 100+Gb/s coherent optical receivers and transmitters. *IEEE J Sel Top Quant Electr*, 20(4):150-157. https://doi.org/10.1109/JSTQE.2013.2295181

Kanazawa S, Kobayashi W, Ueda Y, et al., 2016. 30-km error-free transmission of directly modulated DFB laser array transmitter optical sub-assembly for 100-Gb application. *J Lightw Technol*, 34(15):3646-3652. https://doi.org/10.1109/JLT.2016.2520942

Kang SK, Lee JK, Lee JC, et al., 2010. A compact 4×10-Gb/s CWDM ROSA module for 40G Ethernet optical transceiver. Proc 60th Electronic Components and Technology Conf, p.2001-2005. https://doi.org/10.1109/ECTC.2010.5490670

Li CY, An JM, Zhang JS, et al., 2018. 4×20 GHz silica-based AWG hybrid integrated receiver optical sub-assemblies. *Chin Opt Lett*, 16(6):060603. https://doi.org/10.3788/COL201816.060603

Machado LM, Delrosso G, Borin F, et al., 2014. Advanced optical communication systems and devices. Proc 5th Electronics System-Integration Technology Conf, p.1-4. https://doi.org/10.1109/ESTC.2014.6962752

Ohyama T, Doi Y, Kobayashi W, et al., 2016. Compact hybrid integrated 100-Gb/s transmitter optical sub-assembly using optical butt-coupling between EADFB lasers and silica-based AWG multiplexer. *J Lightw Technol*, 34(3):1038-1046. https://doi.org/10.1109/JLT.2015.2508758

Zhang YS, Liu Y, Lu J, et al., 2017. DFB laser arrays based on the REC technique and their applications in radio-over-fiber systems. *Chin Opt Lett*, 15(1):010005.

Zhang ZK, Liu Y, An JM, et al., 2018. 112 Gbit/s transmitter optical subassembly based on hybrid integrated directly modulated lasers. *Chin Opt Lett*, 16(6):062501.

Zhao ZP, Liu Y, Zhang ZK, et al., 2016. 1.5μm, 8×12.5 Gb/s of hybrid-integrated TOSA with isolators and ROSA for 100 GbE application. *Chin Opt Lett*, 14(12):45-49.

Zhong KP, Zhou X, Huo JH, et al., 2017. Amplifier-less transmission of single channel 112 Gbit/s PAM4 signal over 40km using 25G EML and APD at O band. Proc European Conf on Optical Communication, p.1-3. https://doi.org/10.1109/ECOC.2017.8345975